Bulletin of Engineering Geology and the Environment (2023) 82:455
https://doi.org/10.1007/s10064-023-03476-x

ORIGINAL PAPER

# Influence of confining pressure on permeability and structural properties of selected sedimentary, igneous, and metamorphic rocks

Mateusz Kudasik[1] · Łukasz Anioł[1] · Aleksandra Gajda[1] · Anna Pajdak[1]

Received: 10 April 2023 / Accepted: 6 November 2023 / Published online: 21 November 2023


**Abstract**
As part of the work, studies of the rock's permeability to gases were carried out using the original measuring apparatus, which makes it possible to study gas seepage through a porous medium under confining pressure conditions corresponding to in situ. Samples of selected sandstone, sapropelic coal, marble, granite, limestone, and spongiolite rocks were used for permeability studies. The permeability of these rocks was determined in relation to helium (He) and carbon dioxide ($CO_2$) in various values of the confining pressure: 1, 5, 10, 15, and 30 MPa. The obtained variability ranges of permeability coefficients allowed to assign the tested samples to particular classes, from poor and tight permeable rocks, where $k_\infty < 1$ mD and $k_\infty < 0.1$ mD (granite, marble), through good permeable rocks with a value of $10 < k_\infty < 100$ mD (limestone, spongiolite, sandstone), to very good permeable rocks with coefficient $k_\infty > 100$ mD (coal). The Klinkenberg slippage effect was twice as large for He compared to $CO_2$, and as permeability increased, the slippage effect disappeared. The Walsh model was used to analyze the obtained results, based on which it was found that the highest impact of effective stress was observed for a granite sample, the smallest for sapropelic coal, where an increase in effective stress by about 30 MPa reduced the permeability of coal to He by 50% and to $CO_2$ by 30%. Changes in the structural properties of rocks as a result of subjecting them to gas seepage processes under confining pressure conditions were also examined. Open porosity, specific surface area, pore size distribution, and mean pore diameter in the samples were determined. In most of the studied rocks, a decrease in porosity and a reduction in the pore space of the rocks were observed after permeability tests under confining pressure conditions.

**Keywords** Permeability · Pore structure · Sandstone · Coal · Marble · Granite · Limestone · Spongiolite

## Introduction

Rocks consist of minerals, a solid matrix, and cracks and pores. Pore structure refers to the geometric shape, size, and size distribution of pores and their connectivity, as well as the relationship between all these properties. Pore structure characteristics are influenced by tectonism, sedimentation, and diagenesis. Rock depth is one of the main factors affecting rock integrity and physical properties (Lu et al. 2020). In deeper geological layers, the porosity and permeability of rocks decrease exponentially with increasing depth (Aschwanden et al. 2019). This is mainly due to the confining pressure and stress exerted on the rocks, which increases with the depth of their deposition.

These factors cause deformations and strains that occur in the triaxial stress field. Rocks that have the same mechanical properties in three orthogonal directions are isotropic rocks. They may include, e.g., metamorphic and igneous rocks. Rocks whose properties vary in different directions are anisotropic rocks. Most of them are sedimentary rocks. They are formed as a result of sedimentation, which proceeds gravitationally and its effect is bedding. Anisotropy significantly affects the mechanical strength of rocks, weakening it, which also determines its structural properties and permeability.

Permeability is a parameter that describes the ability of a porous medium to seepage fluids. Most studies on rock permeability show that confining pressure decreases the porosity of rocks, which in turn reduces their permeability to fluids (Konecny and Kozusnikova 2011; Li et al. 2014; Wierzbicki et al. 2014; Zheng et al. 2015; Kudasik 2019; Braga and Kudasik 2019; Estévez-Ventosa et al. 2020; Liu and Spiers 2022). Porosity determines the amount of voids

✉ Mateusz Kudasik
kudasik@imgpan.pl

[1] The Strata Mechanics Research Institute of The Polish Academy of Sciences, Reymonta 27, 30-059 Krakow, Poland

inside the material. Permeability and porosity are basic parameters describing porous media. An attempt to relate porosity and permeability was made almost 100 years ago in the form of the Kozeny-Carman theoretical formula (Kozeny 1927; Carman 1937). Over the years, many theoretical as well as empirical models and indicators, mainly derived from the Kozeny-Carman equation and the Darcy equation, have been developed to relate porosity to rock permeability (Costa 2006). Some theoretical indicators such as FZI, MZI, and RQI have found their application in reservoir quality assessment (Mirzaei-Paiaman et al. 2018). However, in practice, porosity and permeability are considered as two independent parameters in underground hydrodynamics and reservoir engineering (Liu et al. 2019; Bairu et al. 2021).

In situ rock permeability plays a crucial role in (un) conventional geo-energy recovery (such as natural gas/oil, ECBM, shale gas, tight gas/oil, and geothermal energy) (Liu et al. 2011; Sander et al. 2017), mining (Huang et al. 2018; Guo et al. 2021), carbon/waste geological sequestration (Kiyama et al. 2011; Ranjith and Perera 2011), and induced earthquake (Snell et al. 2020).

Under natural conditions, rocks are deposited at considerable depths, often exceeding a thousand meters, where they are loaded by geostatic (confining) pressure, which depends on the density of the overburden rocks and the depth of deposition. The study of energy resources and reservoir rocks under the natural conditions in which these rocks are deposited is extremely complicated, but it can be crucial for assessing the feasibility and effectiveness of their exploitation. Identification of the ability to capture hydrocarbons, crude oil, or mineral resources requires a detailed determination of the properties of these reserves in conditions corresponding to in situ. At geological depths of up to several kilometers, direct measurements of some deposit properties are extremely difficult, economically unjustified, and often even impossible. It is therefore necessary to conduct research on samples collected from these depths and simulate natural conditions in the laboratory.

The permeability of rocks can be reduced several times, or even several dozen times, with the increase in the confining pressure to a value close to the in situ conditions (Pan et al. 2010; Alam et al. 2014; Li et al. 2014). Under the influence of effective stress, the flow channels become narrowed or even completely closed, which in turn significantly reduces the permeability of rocks (Zhijiao et al. 2014). The permeability reduction due to the confining pressure is different for various types of rocks, which have different porosities, structural, physical, and strength properties.

Most permeability studies have been performed on reservoir rocks such as coal (Zhang et al. 2018; Wang et al. 2018; Zhao et al. 2021) or sandstone (Dong et al. 2010; Mohammed 2020; Wang et al. 2022). Typical rock permeabilities studied in various works were in the ranges of 0.1–100 mD for coal (Pan et al. 2010; Braga and Kudasik 2019; Zhao and Wei 2022), 0.4–60 mD for sandstone (Raza et al. 2015), and even about 1000 mD for sandstone with porosity exceeding 20% (Bloch 1991). Much less research on permeability concerns cap rocks, such as shale or limestone (Ghabezloo et al. 2009; Meng et al. 2019), which form layers that isolate the flow of natural gases to upper geological layers. There are also rocks that are considered non-porous and impermeable to gases, such as marble or granite, which are commonly used in the construction industry. The seepage properties of these rocks are usually studied in the context of recognizing the impact of permeability stimulation processes through fracturing (Yang et al. 2017; Ding et al. 2022; Li et al. 2023; Jiao et al. 2023; Ishibashi et al. 2023).

Another group of rocks that have not been tested so far in terms of their permeability are siliceous rocks, such as diatomites and spongiolites (Bus and Karczmarczyk 2014). These rocks are mainly used as sorbents for water and sewage treatment; hence, their seepage properties may be important.

As part of the work, studies of the permeability of several types of rock to helium (He) and carbon dioxide ($CO_2$) were carried out using original apparatus that provides measurements under gas pressure and confining pressure conditions corresponding to in situ. The main purpose of the conducted research was:

- determination of the variability range of permeability coefficients of various types of rocks under confining pressure conditions,
- identification of the range of permeability in which the Klinkenberg slippage effect occurs in various types of rocks and various gases,
- identification of the impact of effective stress on the Walsh fracture permeability of various rocks,
- determination of the influence of permeability and confining pressure on changes in the structural properties of rocks.

## Apparatus

Rock permeability tests were carried out on the original apparatus for seepage, sorption, and exchange sorption test in isobaric conditions, on samples subjected to confining pressure (Kudasik et al. 2020). The apparatus (Figs. 1 and 2) enables measurements to be carried out in isobaric gas and confining pressure conditions as well as in isothermal conditions. The sample to be tested is placed in a high-pressure chamber filled with water, where a confining pressure, regulated in the range of 0–40 MPa, is applied to it. The sample is sealed against water by a rubber coat. Constant confining pressure $p_h$ is ensured by a mechanical actuator, driven by a stepper motor with a gear. Gas ($CO_2$, He) is injected into the sample inlet at a constant $p_{in}$ pressure provided by a pressure regulator. At the sample outlet, the gas flow rate is measured by means of a flow meter. The gas flows into the atmosphere, where the pressure is measured by a barometer $P_{atm}$. The operation of the apparatus and the recording of parameters is carried out by the control system.

## Research material

Rock samples of various origins and physico-chemical properties were used for permeability studies. Sedimentary rocks (sandstones, limestone, coal, spongiolite), igneous rock (granite), and metamorphic rock (marble) were selected. For laboratory permeability tests, samples were prepared in the form of cylindrical rock cores with diameters of about 23–24 mm and lengths of about 40–45 mm. Table 1 presents a description of the tested rocks, and Fig. 3 presents photos of all samples prepared for permeability tests.

## Measurement procedure

Two gases were used to test the permeability of coal samples under confining pressure conditions: helium (He) and carbon dioxide ($CO_2$). The tests were performed at 5 different confining pressures: 1, 5, 10, 15, and 30 MPa. The gas pressure at the sample inlet was regulated in the range of 0.1–1.0 MPa. Rock permeability was determined from Darcy's law:

$$k_g = \frac{2 \bullet Q \bullet p_{atm} \bullet \mu \bullet l}{A \bullet \left({p_{in}}^2 - {p_{atm}}^2\right)}, \quad (1)$$

where $k_g\left[\mathrm{m}^2\right]$—Darcy's permeability coefficient; $Q\left[\frac{\mathrm{m}^3}{\mathrm{s}}\right]$—gas flow at the sample outlet; $p_{atm}$[Pa]—atmospheric pressure; $\mu$[Pa • s]—coefficient of dynamic gas viscosity; $A\left[\mathrm{m}^2\right]$, $l$[m]—sectional area and length of the sample; $p_{in}$[Pa]—gas pressure at the sample inlet.

The permeability described by Darcy's law depends on the fluid pressure in the porous medium. To describe the permeability of the samples under specific conditions of confining pressure, the Klinkenberg correction was used, which describes the absolute permeability of the medium under high gas pressure conditions:

$$k_g = k_\infty \left(1 + \frac{b_k}{p_{avg}}\right), \quad (2)$$

where $k_\infty[\mathrm{m}^2]$—the Klinkenberg's absolute permeability coefficient; $b_k$[Pa]—the Klinkenberg slippage factor, which depends, among other things, on the pore structure of the medium and the mean free path of the gas; $p_{avg}[\mathrm{Pa}] = \frac{p_{in}+p_{atm}}{2}$—average gas pressure.

The method of determining the Klinkenberg permeability coefficients $k_\infty$ and slippage factors $b_k$ was consistent with the methodology presented in the works of (Kudasik 2019), (Braga and Kudasik 2019) and (Kudasik et al. 2022). The procedure for determining permeability coefficients was to measure the gas flow rate $Q$ at the outlet of the sample at different inlet gas pressures $p_{in}$, which flowed through the

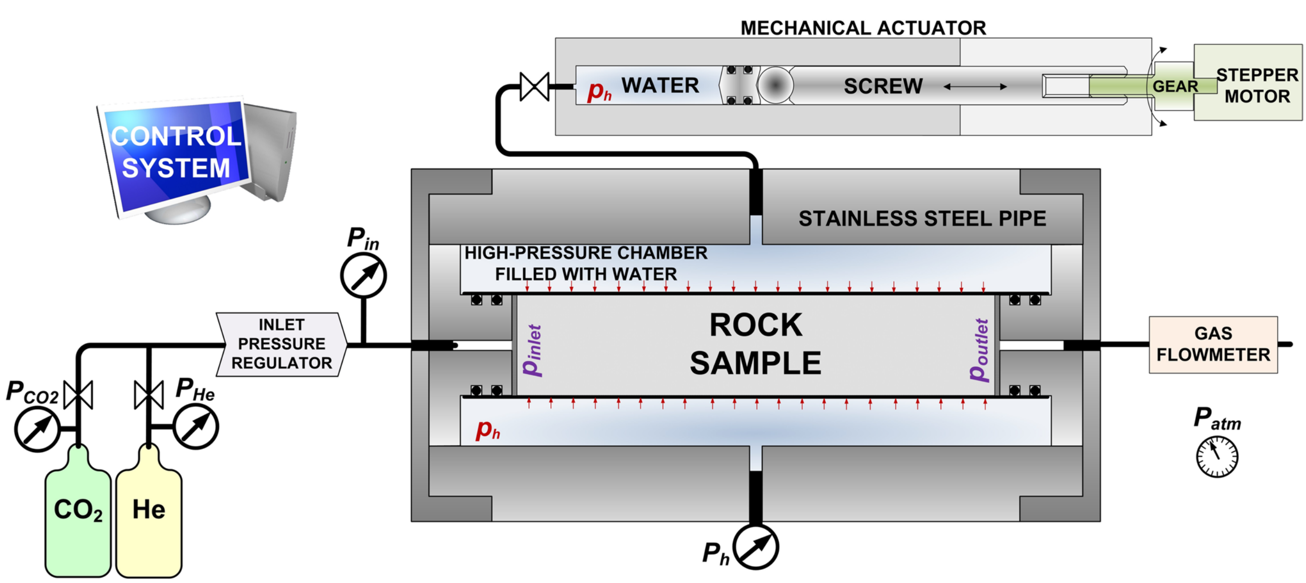


Fig. 1 Scheme of the original apparatus for testing rock permeability under confining pressure conditions

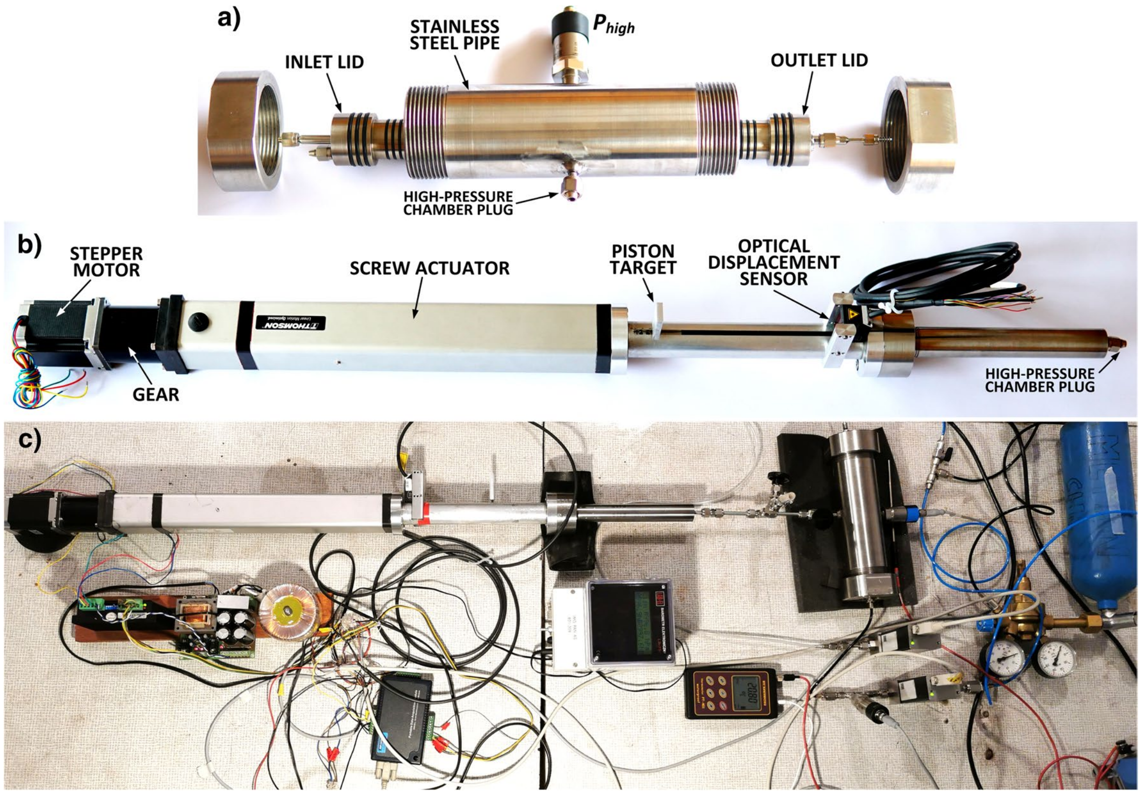


**Fig. 2** Photos of the apparatus for testing rock permeability under confining pressure conditions; **a** high-pressure chamber; **b** a mechanical actuator for generating confining pressure; **c** a complex measuring stand

**Table 1** Origin and description of the studied rocks

| Name, origin | Rock type | Description of the rock/density range/wave velocity range/porosity range |
|---|---|---|
| Sandstone "Tumlin," Poland | Sedimentary rock | A rock composed mainly of silicate sand; it is a reservoir rock; it has high permeability, thanks to which it forms aquifers and oil reservoirs<br>1.61–2.76 g/cm$^3$ / 1.10–1.36 km/s / 10–35% |
| Marble "Supikovice," Czech Republic | Metamorphic rock | A rock composed of recrystallized carbonate minerals, most commonly calcite or dolomite; it is characterized by very low permeability<br>1.9–2.8 g/cm$^3$ / 0.9–1.1 km/s / 0.5–2% |
| Coal "Halemba," Poland | Sedimentary rock | A rock formed as a result of diagenesis and metamorphism of sapropel; It contains the remains of single-celled organisms or plants; compared to hard coal, it contains a significant amount of volatile matter and tar<br>1.1–1.5 g/cm$^3$ / 1.6–2.1 km/s / 4.1–23.2% |
| Spongiolite "Opuka Benatky," Czech Republic | Sedimentary rock | Spongiolite sandy rock; it has the structure of fossilized sponges; it is light and it belongs to the group of organic rocks<br>2.38–2.66 g/cm$^3$ / 2.3–2.8 km/s / 10–35% |
| Granite "Strzelin," Poland | Igneous rock | A rock composed mainly of quartz, alkali feldspar, and plagioclase; it is the most common rock in the earth's crust; due to the lack of pores and impermeability to gases, it is considered as a tap rock<br>2.65– 2.75 g/cm$^3$ / 4.5– 5.5 km/s / 0.4–1.5% |
| Limestone "Czatkowice," Poland | Sedimentary rock | A rock composed mainly of the minerals calcite and aragonite; it is formed by the precipitation of minerals from water containing dissolved calcium; limestone formations cover about 30% of the world's oil reservoirs<br>1.93–2.90 g/cm$^3$ / 2.7–2.95 km/s / 5–16% |

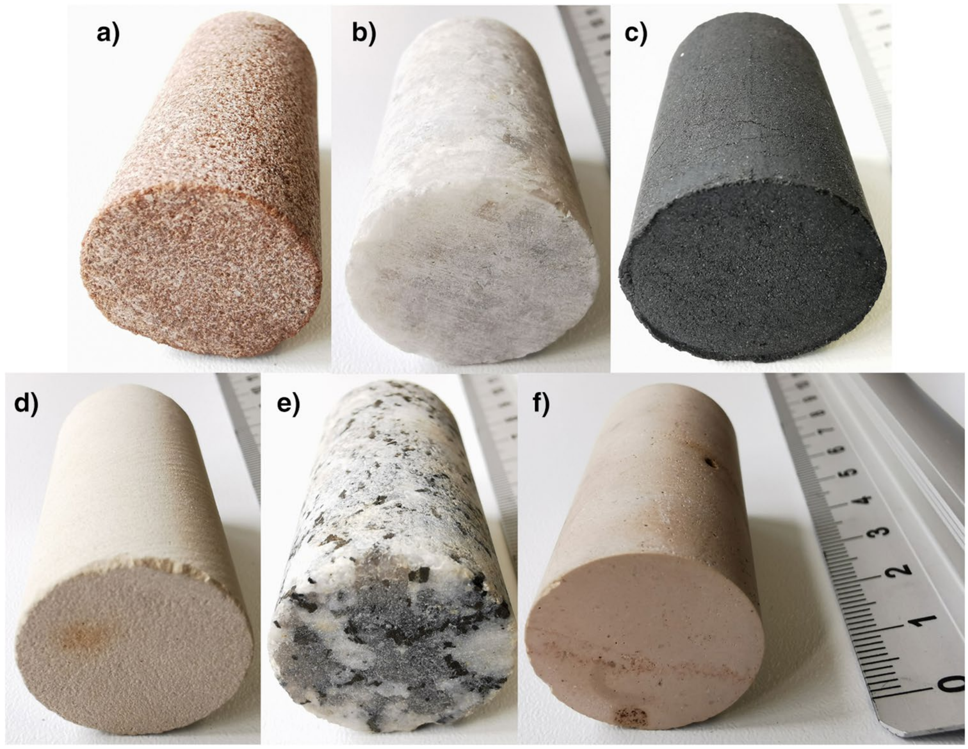


**Fig. 3** Pictures of rock samples: **a** Sandstone "Tumlin"; **b** Marble "Supikovice"; **c** Coal "Halemba"; **d** Spongiolite "Opuka Benatky"; **e** Granite "Strzelin"; **f** Limestone "Czatkowice"

sample into the atmosphere $p_{atm}$. By substituting the values of the parameters $p_{in}$, $p_{atm}$, $Q$ into Eq. (1), the Darcy permeability coefficients were determined. Figure 4 shows schematic diagrams of the changes in the values of the parameters $p_{in}$, $p_{out}$, and $Q$ (Fig. 4a), as well as how the absolute permeability coefficients $k_\infty$ and the Klinkenberg slippage factors $b_k$ (Fig. 4b) were determined, based on the values obtained for these parameters in permeability experiments obtained under different stationary conditions of measurement (P1, P2, P3, P4, and P5). These experiments were repeated at 5 different confining pressures ($p_h$) for both helium (He) and carbon dioxide ($CO_2$).

Both before and after the gas permeability experiments, surface structure parameters, i.e., porosity, specific surface area, and pore volume, were determined in all rock samples. This was to determine the effect of both the confining pressure and the $CO_2$ and He seepage processes on the change of selected structural properties of rocks.

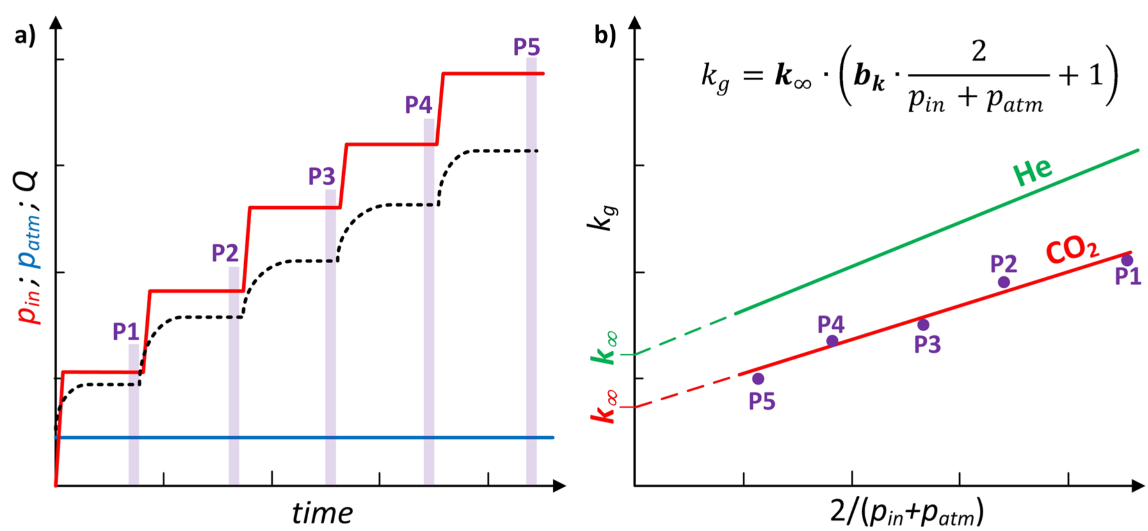


**Fig. 4** Schematic diagrams of the changes in $p_{in}$, $p_{atm}$, and $Q$ parameters during the experiments (**a**), and the methodology for determining the absolute Klinkenberg permeability coefficients $k_\infty$ and Klinkenberg slippage factors $b_k$ (**b**) (Braga and Kudasik 2019; Kudasik et al. 2022)

Porosity was determined using the pycnometic method. The skeletal density of rocks was determined using the AccuPyc II 1340 helium pycnometer (Micromeritics) and the apparent volume using the GeoPyc 1360 quasi-liquid pycnometer (Micromeritics). Before measurement, the samples were heated for 12 h at 378 K. The porosities of the samples were determined before and after permeability measurements.

The surface structure was determined by low-pressure nitrogen adsorption (LPNA) on the ASAP 2020 analyzer (Micromeritics). Nitrogen (N2) adsorption on the surface and in the pore space of granular samples was determined in the pressure range of 0–0.1 MPa and the temperature of 77 K. The measurements were preceded by degassing the samples for 6 h at 378 K under UHV conditions. Based on the nitrogen sorption equilibrium points, the specific surface area of mesopores was determined according to the BET (SBET) (Brunauer 1945) and BJH (SBJH) models (Barrett et al. 1951), as well as the surface area of micropores according to the DFT (SDFT) theory (Duda et al. 2007). The volume of available pores (VBJH, VDFT) and their average size (DBJH) were determined based on BJH and DFT models.

## Results

### Klinkenberg permeability

Description of the permeability of porous media characterized by low porosity and permeability, in particular under stress conditions, the Klinkenberg permeability model (2) is used. This model takes into account the occurrence of the Klinkenberg slippage effect, which occurs on the pore walls

**Table 2** Values of the absolute permeability coefficients $k_\infty$ and the Klinkenberg slippage factors $b_k$ at different confining pressures

| Sample | Confining pressure $p_h$ [MPa] | Klinkneberg permeability and slippage factors in relation to: | | | |
|---|---|---|---|---|---|
| | | He | | $CO_2$ | |
| | | $k_\infty$[mD] | $b_k$[MPa] | $k_\infty$[mD] | $b_k$[MPa] |
| Sandstone “Tumlin” | 1 | 129.59 | 0.27 | 99.44 | 0.04 |
| | 5 | 73.69 | 0.48 | 60.20 | 0.16 |
| | 10 | 53.17 | 0.67 | 51.53 | 0.14 |
| | 15 | 51.82 | 0.62 | 52.84 | 0.12 |
| | 30 | 49.46 | 0.48 | 40.43 | 0.17 |
| Marble “Supikovice” | 1 | 0.24 | 1.14 | 0.12 | 0.33 |
| | 5 | 0.16 | 1.02 | 0.03 | 1.28 |
| | 10 | 0.09 | 1.54 | 0 | 0 |
| | 15 | 0.04 | 0.23 | 0 | 0 |
| | 30 | 0 | 0 | 0 | 0 |
| Coal “Halemba” | 1 | 446.43 | 0 | 176.61 | 0 |
| | 5 | 302.29 | 0 | 162.51 | 0 |
| | 10 | 275.40 | 0 | 150.81 | 0 |
| | 15 | 258.34 | 0 | 143.61 | 0 |
| | 30 | 217.37 | 0 | 125.64 | 0 |
| Spongiolite “Opuka Benatky” | 1 | 381.47 | 0.03 | 101.03 | 0.08 |
| | 5 | 89.13 | 0.38 | 78.19 | 0.18 |
| | 10 | 49.58 | 0.57 | 36.20 | 0.20 |
| | 15 | 42.37 | 0.60 | 31.74 | 0.24 |
| | 30 | 20.91 | 1.05 | 17.46 | 0.26 |
| Granite “Strzelin” | 1 | 4.98 | 0.30 | 3.21 | 0.69 |
| | 5 | 0.41 | 0.88 | 0.14 | 1.23 |
| | 10 | 0.28 | 1.52 | 0.06 | 1.48 |
| | 15 | 0.01 | 1.82 | 0 | 1.20 |
| | 30 | 0 | 0 | 0 | 0 |
| Limestone “Czatkowice” | 1 | 25.31 | 1.11 | 19.15 | 0.06 |
| | 5 | 22.53 | 1.40 | 9.99 | 0.32 |
| | 10 | 20.58 | 1.70 | 6.78 | 0.49 |
| | 15 | 19.30 | 1.70 | 5.56 | 0.53 |
| | 30 | 17.30 | 1.69 | 5.23 | 0.47 |

as the gas flows through the smallest pores (Wu et al. 1998; Tanikawa and Shimamoto 2006).

Based on the measurement results, the absolute permeability coefficients $k_\infty$ and the Klinkenberg slippage factors $b_k$ of all samples were determined, at 5 different confining pressures and for two gases (He and $CO_2$). The values of the determined coefficients are presented in Table 2.

Based on the study, it was observed that an increase in confining pressure induces a decrease in rock permeability to He and $CO_2$. In addition, the permeability of all rocks to He was higher than to $CO_2$, which results, among others, from the difference in particle size of both gases, where the kinetic diameter of He is 0.26 nm and the kinetic diameter of $CO_2$ is 0.33 nm.

The Klinkenberg slippage effect occurs in gas flows through small pores; hence, as porosity, and therefore rock permeability, increases, this effect should disappear. To investigate this relationship, a graph of changes in slippage factors $b_k$ as a function of the permeability $k_\infty$ of all samples to He and $CO_2$, was drawn (Fig. 5). These relationships were fitted by an exponential equation, on the basis of which it can be concluded that the Klinkenberg slippage effect is almost twice as large for He as for $CO_2$. In the tests with the use of $CO_2$, at permeability of rock samples above 120 mD, the value of the $b_k$ factor was 0, while in the tests of permeability to He, the slippage effect disappeared for $k_\infty$ above 220 mD. Hence, it can be concluded that the Klinkenberg slippage effect is mainly dependent on the permeability and the type of gas. The type of rock, in turn, has only an indirect impact on the occurrence of the Klinkenberg slippage effect, as the direct influence is due to its porosity and permeability.

The Klinkenberg slippage effect is highest at the lowest permeabilities which can be explained by the fact that gas flow in the smallest pores is affected by Knudsen diffusion, which contributes to an increase in the slippage of gas molecules on the pore walls. As a result, when gas flows through pores that are similar in size to the gas particles, the mean free path decreases causing slippage and an increase in flow rate.

Comparison of rock permeability to He and $CO_2$ is shown in Fig. 6, where the tested rocks were also assigned to appropriate groups, according to the classification proposed by (Abuamarah et al. 2019). The sapropelic coal sample had the highest permeability coefficients of up to 446 mD and was classified as a very good permeable rock. The group of good permeable rocks includes samples of spongiolite, sandstone, and limestone. The lowest permeability was found in marble and granite samples, which were classified as tight permeability rocks under confining pressure conditions. This classification can be closely related to the porosities of the samples (Table 1), where coal and spongiolite samples had the highest values (38.40% and 45.69%), followed by sandstone and marble (10.37% and 6.80%), and limestone and granite samples had the lowest porosities (1.93% and 1.92%). Of course, these porosities were reduced during the course of the measurement, as a result of increasing confining pressure.

## Walsh fracture permeability

Using the Walsh permeability model (Walsh 1981), one can describe the variation of the fracture permeability ($\kappa$) between two rough surfaces with respect to the change in applied effective stress:

$$\frac{\kappa}{\kappa_0} = \left[1 - a \bullet ln\left(\frac{\sigma_e}{\sigma_{e0}}\right)\right]^3 \bullet \left[\frac{1 - b \bullet \left(\sigma_e - \sigma_{e0}\right)}{1 + b \bullet \left(\sigma_e - \sigma_{e0}\right)}\right], \quad (3)$$

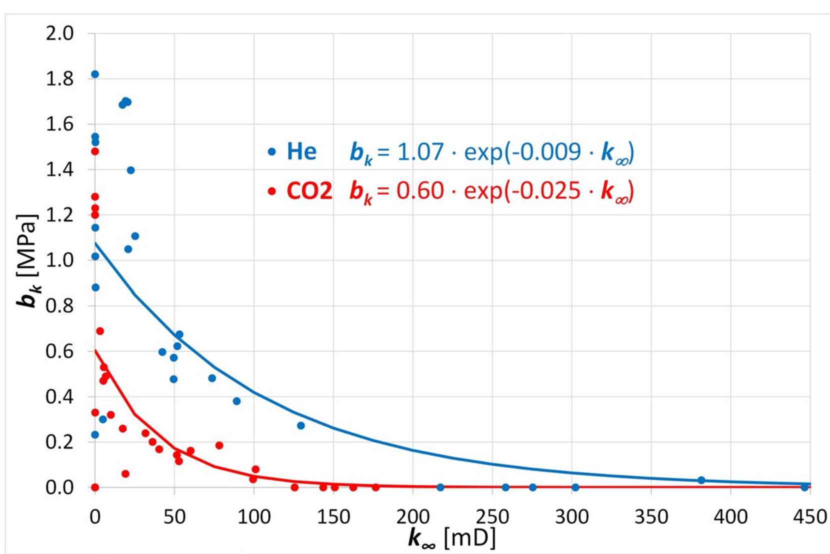


**Fig. 5** Dependence of slippage factors $b_k$ on Klinkenberg permeability coefficients $k_\infty$

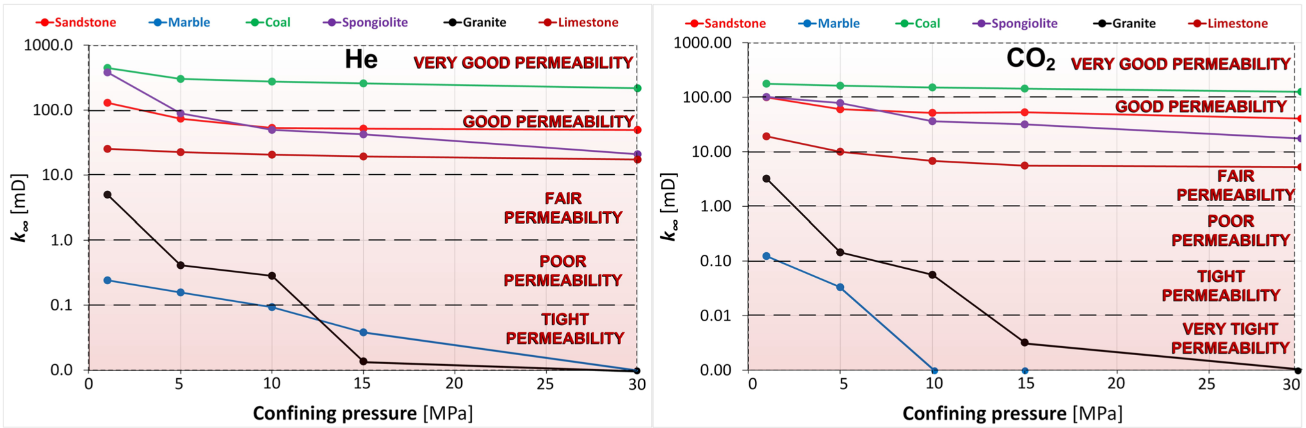


**Fig. 6** Classification of the studied rocks in terms of their permeability to He and $CO_2$

where $\kappa\,[\mathrm{m}^2]$—fracture permeability; $\sigma_e = (p_h - s \bullet p_{avg})$ [MPa]—effective stress, $s\,[-]$—effective Walsh stress factor; $\kappa_0\,[\mathrm{m}^2]$, $\sigma_{e0}$ [MPa]—reference permeability and reference effective stress; $a = 2\sqrt{2} \bullet \left(\frac{h}{D_0}\right)$—reflects the physical properties of the fracture, where $h$[m] is the root mean square value of the fracture surface height distribution and $D_0$[m] is the mean fracture width at reference effective stresses $\sigma_{e0}$ and permeability $\kappa_0$; $b\left[\mathrm{MPa}^{-1}\right]$—constant for Hertzian contact.

Based on the rock permeability test results (Table 2), the dependence of the Walsh fracture permeability on the effective stress can be determined by fitting Eq. (3) to the measurement points. The Walsh equation obtained in this way enables to describe the structure of the gas flow fracture under the effective stress conditions (Table 3).

Based on the determined parameters of the Walsh Eq. (3), model changes in fracture permeability were plotted by fitting them to the measurement points (Fig. 7).

One of the benefits of using the Walsh model is the ability to qualitatively and quantitatively determine the impact of effective stress on permeability (Zhang et al. 2016; Chen et al. 2016). By plotting the quotient of the fracture permeability to the reference permeability $\left(\frac{\kappa}{\kappa_0}\right)$ and the effective stress (Fig. 8), it is possible to observe for which sample the influence of the effective stress on the permeability was the highest.

Based on the obtained results, it was found that the highest impact of effective stress was observed for the granite sample, both in tests using He and $CO_2$. This was shown by the highest decrease in the relative permeability value $\frac{\kappa}{\kappa_0}$, where at an effective stress above 10 MPa, the permeability of the granite sample was reduced by 100% relative to the reference value $\kappa_0$, corresponding to $\sigma_{e0}$= 0.65 MPa. In turn, the smallest effect of the effective stress was observed for the sapropelic coal sample, for which the effective stress of 30 MPa reduced its permeability by about 50% in relation to He and about 30% in relation to $CO_2$.

The Walsh model is a commonly used solution to describe the fracture permeability-stress relationship. The fit obtained with it enables the determination of parameters describing the physical properties of the flow fracture. However, when the seepage process is dominated within the micro-, meso-, and macropores, the Walsh model is rarely used.

## Structural properties

The pore structure of the rocks was determined on the basis of nitrogen adsorption equilibrium points (LPNA). The isotherms fitted to these adsorption equilibrium points had the shapes of type III isotherms for all rocks, which are characteristic of low-porous and non-porous materials.

**Table 3** Values of Walsh fracture permeability Eq. (3) parameters for all tested samples

| Sample | Gas | $a[-]$ | $b[-]$ | $\kappa_0$[mD] | $\sigma_{e0}$[MPa] |
|---|---|---|---|---|---|
| Sandstone "Tumlin" | He | 0.088 | 0 | 129.6 | 0.75 |
| | $CO_2$ | 0.071 | 0 | 99.4 | 0.71 |
| Marble "Supikovice" | He | 0.036 | 0.034 | 0.241 | 0.56 |
| | $CO_2$ | 0.128 | 0.066 | 0.123 | 0.56 |
| Coal "Halemba" | He | 0.062 | 0 | 446.4 | 0.87 |
| | $CO_2$ | 0.011 | 0.004 | 176.6 | 0.88 |
| Spongiolite "Opuka Benatky" | He | 0.183 | 0 | 357.8 | 0.71 |
| | $CO_2$ | 0.038 | 0.023 | 101.0 | 0.63 |
| Granite "Strzelin" | He | 0.267 | 0.018 | 4.98 | 0.65 |
| | $CO_2$ | 0.298 | 0.059 | 3.21 | 0.65 |
| Limestone "Czatkowice" | He | 0.016 | 0.003 | 25.3 | 0.55 |
| | $CO_2$ | 0.097 | 0 | 19.1 | 0.55 |

For most samples, the adsorption/desorption isotherm before and after the permeability tests had a similar shape and hysteresis loops with a small area were obtained. The total adsorption capacity at $p/p_0=1$ varied for different rocks (Fig. 9). The lowest values of $N_2$ adsorption isotherm parameters were obtained for coal, marble, and granite samples (Fig. 8a). In these samples, the $N_2$ adsorption isotherms before and after the permeability tests under confining pressure conditions did not differ significantly. The maximum adsorption capacity in the initial samples was 0.16–0.22 cm$^3$/g, and after the permeability tests it was 0.16–0.43 cm$^3$/g. In the samples of limestone, spongiolite, and sandstone, higher values of the adsorption capacity with respect to $N_2$ were obtained (Fig. 8b). In the initial samples of limestone and sandstone, the adsorption capacity was 3.0–4.5 cm$^3$/g and after the permeability tests it did not change significantly (3.2–3.7 cm$^3$/g). In the spongiolite sample, before the measurement, the highest adsorption capacity was obtained—74.5 cm$^3$/g, while after the permeability measurements, it was significantly reduced to 6 cm$^3$/g.

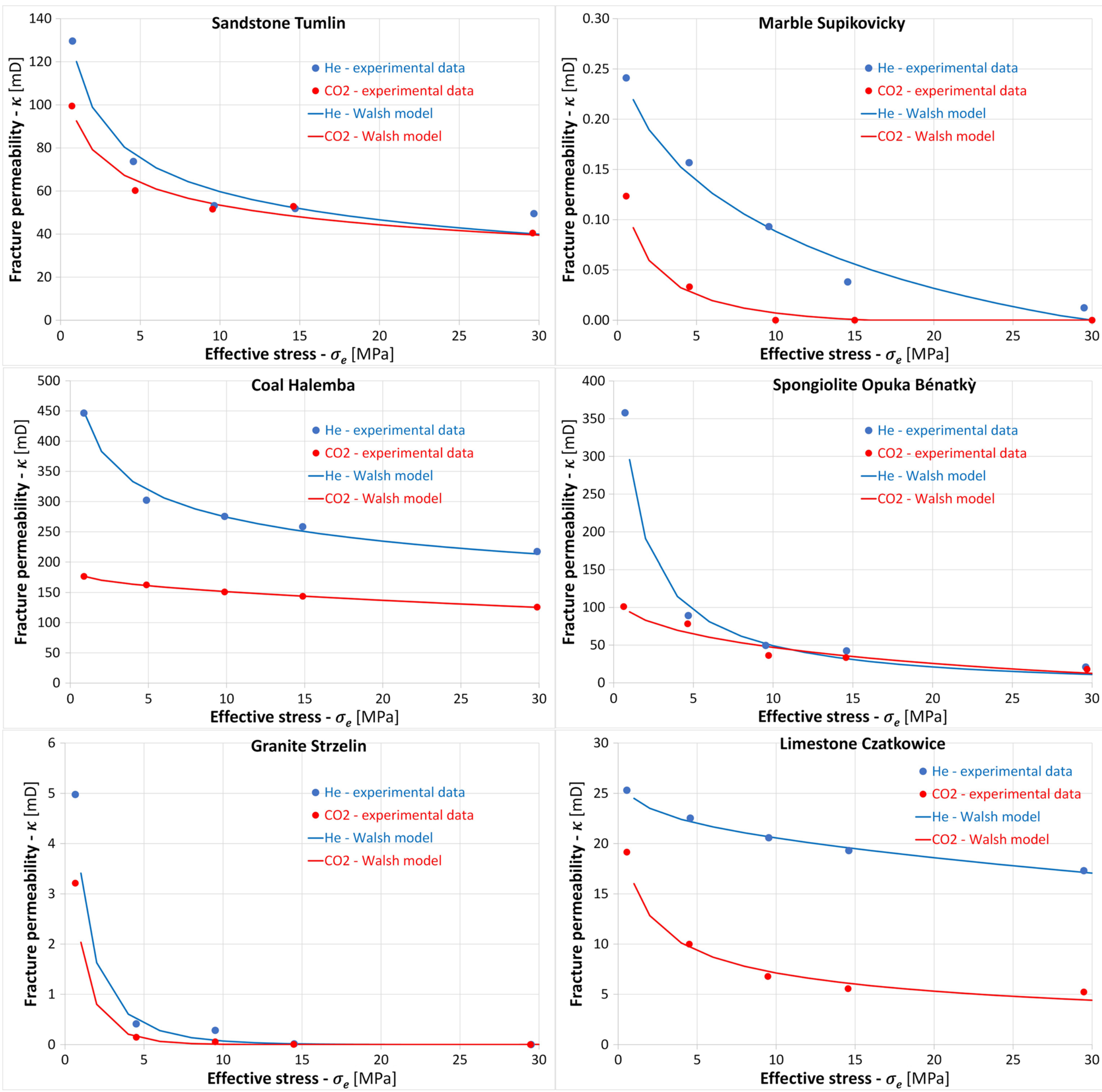


**Fig. 7** Changes in the Walsh fracture permeability of rocks to He and $CO_2$

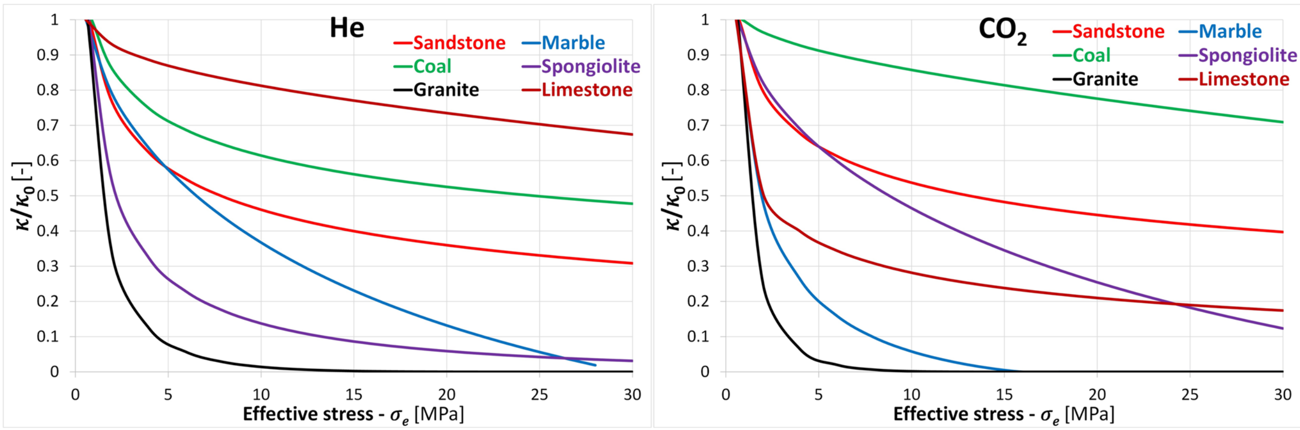


**Fig. 8** The dependence of the change of the Walsh fracture permeability in relation to the reference permeability $\left(\frac{\kappa}{\kappa_0}\right)$ on the effective stress for all samples

Based on the determined sorption isotherm, the structural parameters were determined. For most of the samples, the BET- and BJH-specific surface area parameters (mesopore range) slightly decreased or did not change after the permeability tests. In spongiolite and sandstone samples, the decrease in these parameters was significant. In spongiolite, the specific surface area was reduced from 22 to 26 m$^2$/g to about 2 m$^2$/g, after permeability tests at confining pressure of up to 30 MPa. The microporous specific surface area decreased from 12 m$^2$/g by nearly one order of magnitude, as did the volume of available pores. In the remaining rocks, the available surface area of micropores and the volume of pores was slightly reduced.

The confining pressure had a high impact on the porosity of the tested rocks (Table 4). A reduction in the porosity of each sample was observed, with the highest decrease measured for the spongiolite sample and it ranged from 45.7% before permeability tests to 10.2% after permeability tests at confining pressures of up to 30 MPa. A more than two-fold decrease in porosity was observed for limestone and granite, from 6.8 to 2.9% and from 1.9 to 0.8%, respectively. The porosities of the remaining rocks decreased relatively to 10% of the initial value.

## Conclusions

Rock is a geological discontinuous material that contains solid components with varying values of density, compressive strength, and solubility, as well as containing pore voids and fractures. These pores may be filled with a fluid of various properties, which may not be inert to the rocks. This paper investigates the effect of confining pressure

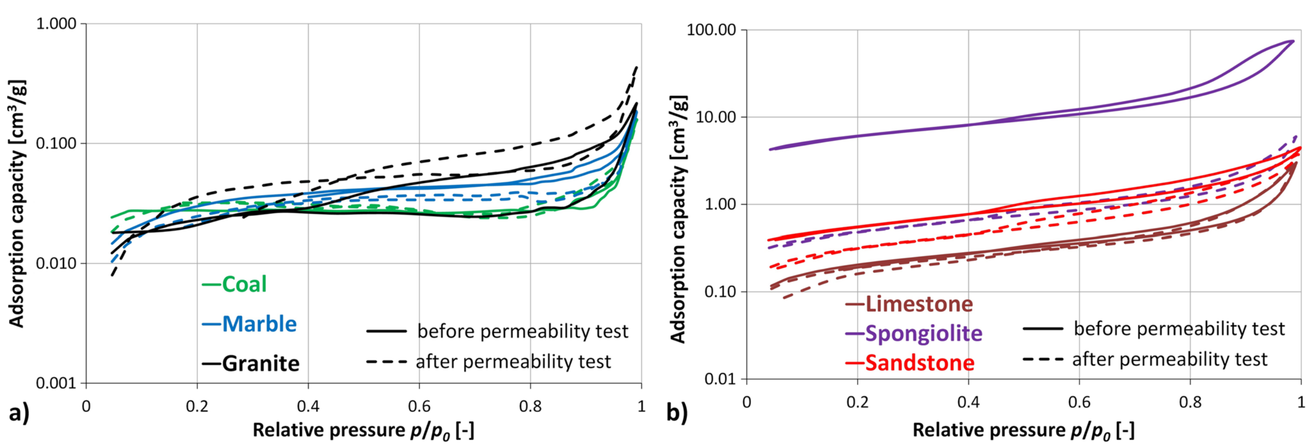


**Fig. 9** $N_2$ adsorption capacities of various rocks before and after permeability tests under confining pressure conditions: **a** a group of rocks with low adsorption capacities; **b** a group of rocks with higher adsorption capacities

**Table 4** Results of structural studies of rocks

| Sample | Before/after permeability tests | $\varnothing_o$ [%] | $a_1$ [cm$^3$/g] | $S_{BET}$ [m$^2$/g] | $S_{BJH}$ [m$^2$/g] | $V_{BJH}$ [mm$^3$/g] | $D_{BJH}$ [nm] | $S_{DFT}$ [m$^2$/g] | $V_{DFT}$ [mm$^3$/g] |
|---|---|---|---|---|---|---|---|---|---|
| Sandstone "Tumlin" | Before | 10.37 | 4.48 | 2.06 | 2.39 | 4.37 | 11.7 | 1.07 | 2.24 |
| | After | 9.73 | 3.73 | 1.24 | 1.55 | 5.75 | 14.8 | 0.76 | 1.93 |
| Marble "Supikovice" | Before | 1.93 | 0.18 | 0.12 | 0.13 | 0.28 | 8.7 | 0.03 | 0.08 |
| | After | 1.32 | 0.18 | 0.11 | 0.11 | 0.28 | 10.6 | 0.04 | 0.06 |
| Coal "Halemba" | Before | 38.40 | 0.16 | 0.10 | 0.02 | 0.19 | 48.4 | 0.00 | 0.03 |
| | After | 36.49 | 0.16 | 0.10 | 0.02 | 0.18 | 45.8 | 0.01 | 0.04 |
| Spongiolite "Opuka Benatky" | Before | 45.69 | 74.47 | 22.20 | 26.42 | 113.1 | 17.1 | 11.78 | 37.59 |
| | After | 10.20 | 5.97 | 1.81 | 2.05 | 8.92 | 17.43 | 0.89 | 2.52 |
| Granite "Strzelin" | Before | 1.92 | 0.22 | 0.09 | 0.07 | 3.12 | 18.0 | 0.02 | 0.04 |
| | After | 0.79 | 0.43 | 0.22 | 0.10 | 0.60 | 25.4 | 0.10 | 0.06 |
| Limestone "Czatkowice" | Before | 6.80 | 3.01 | 0.79 | 0.84 | 4.37 | 20.8 | 0.47 | 0.48 |
| | After | 2.85 | 3.21 | 0.72 | 0.77 | 4.68 | 24.3 | 0.48 | 0.44 |

where $\varnothing_o$—open porosity; $a_1$—sorption capacity at relative pressure $p/p_0 = 1$; $S_{BET}$—specific surface area BET; $S_{BJH}$—specific surface area BJH; $V_{BJH}$—mesopore volume BJH; $D_{BJH}$—average pore diameter BJH; $S_{DFT}$—specific surface area of micropores DFT; $V_{DFT}$—micropore volume DFT

on permeability to two gases (He and $CO_2$) with different physical and chemical properties. Experiments were performed on 6 different rocks on the original measuring apparatus. Based on the experiments performed, the following conclusions can be drawn:

- The sapropelic coal sample had the highest permeability of up to 446 mD in relation to He and was classified as a very good permeable rock. The group of good permeable rocks included samples of spongiolite, sandstone, and limestone. The lowest permeability in relation to both gases was found in marble and granite samples, which were classified as poor and tight permeable rocks with coefficients below 1 mD and 0.1 mD under confining pressure conditions.
- The Klinkenberg slippage effect was almost twice as large for He than for $CO_2$ and disappeared at gas permeability coefficients above 120 mD for all samples.
- The highest impact of the effective stress was observed for the granite sample, both in tests using He and $CO_2$, where at the effective stress above 10 MPa, the permeability of the granite was reduced by 100%. The smallest impact of effective stress was observed for the coal sample, where at a stress of 30 MPa permeability decreased by about 50% in measurements with He and by about 30% in measurements with $CO_2$.
- Based on the LPNA isotherm and the values of structural parameters, the rocks were classified as low-porous and non-porous. The porosity of the samples ranged from a few to over a dozen percent. Only in the samples of spongiolite and sapropelic coal the value of porosity was much higher, in the range of 36–46%.
- In most rocks, the effect of the confining pressure caused a slight change in the value of the specific surface area and the volume of available pores. Only in the spongiolite the structural parameters were significantly reduced. The pores were closed and the specific surface area decreased. The reduction of porosity and other structural parameters of the rocks was mainly due to the confining pressure reaching 30 MPa during permeability measurements. Another cause of changes in structural parameters, but with a much smaller impact, was the reaction with $CO_2$.
- The studied sedimentary rocks—sandstones, limestones, and spongiolite—are subject to anisotropic stresses in their natural state, which have different properties in different directions. This is due to the sedimentation that occurs gravitationally during the formation of these rocks. The consequences of this process are faulting, discontinuities, and cracks in the structure of the rock. Experiments under confining pressure conditions permanently altered the structure of these rocks. In particular, in spongiolite and limestone, porosity decreased by 78% and 59%, respectively. In sandstone, there was a smaller change in porosity—by 7%—and a 40% decrease in BET surface area and pore volume was observed.
- The metamorphic rock—marble—had very similar structural properties before and after the experiments. This was due to the fact that, under in situ conditions, the marble is subject to isotropic stresses that are similar in all three XYZ directions.
- In sapropelic coal, the values of changes in porosity and structural parameters were negligible. A decrease in the porosity value of only 5% was observed. This was due to the fact that sapropel coal has small pores in its structure,

which are elastic. Thus, in the context of the nature of rock deformation, it is an elastic rock and is characterized by the ability to continuous deformation.

- In the tested granite, which has a brittle nature in the context of rock deformation, fractures appeared as a result of the experiments. The porosity value and pore volume (BJH) were significantly reduced after the experiment by 59% and 81%, respectively.

The results of comprehensive studies performed under confining pressure conditions represent an innovative approach to the subject of rock permeability. The experiments were carried out on a unique, original apparatus that enables the determination of permeability parameters with high sensitivity and accuracy. Simulation of conditions corresponding in situ enables observation of processes occurring in pore space and fractures during gas flow. Both sedimentary, magmatic, and metamorphic rocks were used in the study. These rocks were classified into appropriate groups based on permeability, and the effects of stress and gas transport on the structure of these rocks were characterized. The results presented in this article can be a source of knowledge not only in the context of permeability and structural properties of rocks in situ, but also provide information on the correlation between these parameters. Therefore, they are extremely valuable from the application point of view.

**Acknowledgements** The work was carried out at the Strata Mechanics Research Institute of the Polish Academy of Sciences as part of statutory work financed by the Ministry of Education and Science.

**Funding** Ministry of Education and Science (Poland)

**Data availability** Data supporting the study results are available from the authors, but there are restrictions on the availability of this data, which was used under license from The Strata Mechanics Research Institute of the Polish Academy of Sciences for the purposes of the current study and is therefore not publicly available. However, the data are made available by the authors upon request and with the consent of The Strata Mechanics Research Institute of the Polish Academy of Sciences.

## Declarations

**Conflict of interest** The authors declare no competing interests.



## References

Abuamarah BA, Nabawy BS, Shehata AM et al (2019) Integrated geological and petrophysical characterization of oligocene deep marine unconventional poor to tight sandstone gas reservoir. Mar Pet Geol 109:868–885. https://doi.org/10.1016/j.marpetgeo.2019.06.037

Alam AKMB, Niioka M, Fujii Y et al (2014) Effects of confining pressure on the permeability of three rock types under compression. Int J Rock Mech Min Sci 65:49–61. https://doi.org/10.1016/j.ijrmms.2013.11.006

Aschwanden L, Diamond LW, Adams A (2019) Effects of progressive burial on matrix porosity and permeability of dolostones in the foreland basin of the Alpine Orogen, Switzerland. Mar Pet Geol 100:148–164. https://doi.org/10.1016/j.marpetgeo.2018.10.055

Bairu Z, Yang S, Beining W, Yonggi L (2021) Experimental study on the effects of vibrational frequency on the permeability of gas-containing coal rocks. Arch Min Sci 66:265–278. https://doi.org/10.24425/ams.2021.137461

Barrett EP, Joyner LG, Halenda PP (1951) The determination of pore volume and area distributions in porous substances. I. Computations from Nitrogen Isotherms. J Am Chem Soc 73:373–380. https://doi.org/10.1021/ja01145a126

Bloch S (1991) Empirical prediction of porosity and permeability in sandstones (1). Am Assoc Pet Geol Bull 75:1145–1160. https://doi.org/10.1306/0C9B28E9-1710-11D7-8645000102C1865D

Braga LTP, Kudasik M (2019) Permeability measurements of raw and briquette coal of various porosities at different temperatures. Mater Res Express 6:105609. https://doi.org/10.1088/2053-1591/ab39fe

Brunauer S (1945) The Adsorption of Gases and Vapors. Princeton University Press 1

Bus A, Karczmarczyk A (2014) Properties of lime-siliceous rock opoka as reactive material to remove phosphorous from water and wastewater. Infrastruct Ecol Rural Areas 2:227–238

Carman PC (1937) Fluid flow through granular beds. Trans Inst Chem Eng Lond 15:150–156

Chen D, Pan Z, Ye Z et al (2016) A unified permeability and effective stress relationship for porous and fractured reservoir rocks. J Nat Gas Sci Eng 29:401–412. https://doi.org/10.1016/j.jngse.2016.01.034

Costa A (2006) Permeability-porosity relationship: a reexamination of the Kozeny-Carman equation based on a fractal pore-space geometry assumption. Geophys Res Lett 33:L02318. https://doi.org/10.1029/2005GL025134

Ding Q-L, Wang P, Cheng Z (2022) Permeability evolution of fractured granite after exposure to different high-temperature treatments. J Pet Sci Eng 208:109632. https://doi.org/10.1016/j.petrol.2021.109632

Dong J-J, Hsu J-Y, Wu W-J et al (2010) Stress-dependence of the permeability and porosity of sandstone and shale from TCDP Hole-A. Int J Rock Mech Min Sci 47:1141–1157. https://doi.org/10.1016/j.ijrmms.2010.06.019

Duda JT, Jagiełło L, Jagiełło J, Milewska-Duda J (2007) Complementary study of microporous adsorbents with DFT and LBET. Appl Surf Sci 253:5616–5621. https://doi.org/10.1016/j.apsusc.2006.12.100

Estévez-Ventosa X, González-Molano NA, Blázquez-Pascual V et al (2020) A methodology to estimate permeability in porous and fissured rock specimens at laboratory scale. Arch Min Sci 65:821–833. https://doi.org/10.24425/ams.2020.135179

Ghabezloo S, Sulem J, Guédon S, Martineau F (2009) Effective stress law for the permeability of a limestone. Int J Rock Mech Min Sci 46:297–306. https://doi.org/10.1016/j.ijrmms.2008.05.006

Guo H, Tang H, Wu Y et al (2021) Gas seepage in underground coal seams: application of the equivalent scale of coal matrix-fracture structures in coal permeability measurements. Fuel 288:119641. https://doi.org/10.1016/j.fuel.2020.119641

Huang Q, Wu B, Cheng W et al (2018) Investigation of permeability evolution in the lower slice during thick seam slicing mining and gas drainage: a case study from the Dahuangshan coalmine in China. J Nat Gas Sci Eng 52:141–154. https://doi.org/10.1016/j.jngse.2018.01.036

Ishibashi T, Asanuma H, Mukuhira Y, Watanabe N (2023) Laboratory hydraulic shearing of granitic fractures with surface roughness under stress states of EGS: permeability changes and energy balance. Int J Rock Mech Min Sci 170:105512. https://doi.org/10.1016/j.ijrmms.2023.105512

Jiao Y, Wang Y, Feng D et al (2023) Laboratory study on fluid-induced fracture slip and permeability evolution in marble fractures. Rock Mech Rock Eng 56:2497–2513. https://doi.org/10.1007/s00603-022-03168-0

Kiyama T, Nishimoto S, Fujioka M et al (2011) Coal swelling strain and permeability change with injecting liquid/supercritical CO2 and N2 at stress-constrained conditions. Int J Coal Geol 85:56–64. https://doi.org/10.1016/j.coal.2010.09.010

Konecny P, Kozusnikova A (2011) Influence of stress on the permeability of coal and sedimentary rocks of the Upper Silesian basin. Int J Rock Mech Min Sci 48:347–352. https://doi.org/10.1016/j.ijrmms.2010.11.017

Kozeny J (1927) Über kapillare Leitung der Wassers im Boden. Akademie Der Wissenschaften Wien 136:271–306

Kudasik M (2019) Investigating permeability of coal samples of various porosities under stress conditions. Energies (basel) 12:762. https://doi.org/10.3390/en12040762

Kudasik M, Skoczylas N, Pajdak A (2020) Innovative apparatus for testing filtration, sorption and CO2/CH4 exchange sorption processes under isobaric conditions on sorbent subjected to confining pressure in terms of laboratory tests of CO2-ECBM technology. Sensors 20:5823. https://doi.org/10.3390/s20205823

Kudasik M, Skoczylas N, Braga LTP (2022) laboratory studies on permeability of coals using briquettes: understanding underground storage of CO2. Energies (basel) 15:715. https://doi.org/10.3390/en15030715

Li Y, Tang D, Xu H et al (2014) Experimental research on coal permeability: the roles of effective stress and gas slippage. J Nat Gas Sci Eng 21:481–488. https://doi.org/10.1016/j.jngse.2014.09.004

Li Z, Ma X, Kong X-Z et al (2023) Permeability evolution during pressure-controlled shear slip in saw-cut and natural granite fractures. Rock Mech Bull 2:100027. https://doi.org/10.1016/j.rockmb.2022.100027

Liu J, Chen Z, Elsworth D et al (2011) Interactions of multiple processes during CBM extraction: A critical review. Int J Coal Geol 87:175–189. https://doi.org/10.1016/j.coal.2011.06.004

Liu Z, Zhong X, Qin B et al (2019) Redevelopment of fractures and permeability changes after multi-seam mining of shallow closely spaced coal seams. Arch Min Sci 64:671–686. https://doi.org/10.24425/ams.2019.129376

Liu J, Spiers CJ (2022) Permeability of bituminous coal to CH4 and CO2 under fixed volume and fixed stress boundary conditions: effects of sorption. Front Earth Sci (Lausanne) 10. https://doi.org/10.3389/feart.2022.877024

Lu Y, Li C, He Z et al (2020) Variations in the physical and mechanical properties of rocks from different depths in the Songliao Basin under uniaxial compression conditions. Geomech Geophys Geo-Energy Geo-Resources 6:43. https://doi.org/10.1007/s40948-020-00163-z

Meng F, Baud P, Ge H, Wong T (2019) The effect of stress on limestone permeability and effective stress behavior of damaged samples. J Geophys Res Solid Earth 124:376–399. https://doi.org/10.1029/2018JB016526

Mirzaei-Paiaman A, Ostadhassan M, Rezaee R et al (2018) A new approach in petrophysical rock typing. J Pet Sci Eng 166:445–464. https://doi.org/10.1016/j.petrol.2018.03.075

Mohammed AKA (2020) A review: controls on sandstone permeability during burial and its measurements comparison—example, Permian Rotliegend Sandstone. Model Earth Syst Environ 6:591–603. https://doi.org/10.1007/s40808-019-00704-w

Pan Z, Connell LD, Camilleri M (2010) Laboratory characterisation of coal reservoir permeability for primary and enhanced coalbed methane recovery. Int J Coal Geol 82:252–261. https://doi.org/10.1016/j.coal.2009.10.019

Ranjith PG, Perera MSA (2011) A new triaxial apparatus to study the mechanical and fluid flow aspects of carbon dioxide sequestration in geological formations. Fuel 90:2751–2759. https://doi.org/10.1016/j.fuel.2011.04.004

Raza A, Bing CH, Nagarajan R, Hamid MA (2015) Experimental investigation on sandstone rock permeability of Pakistan gas fields. IOP Conf Ser Mater Sci Eng 78:012007. https://doi.org/10.1088/1757-899X/78/1/012007

Sander R, Pan Z, Connell LD (2017) Laboratory measurement of low permeability unconventional gas reservoir rocks: A review of experimental methods. J Nat Gas Sci Eng 37:248–279. https://doi.org/10.1016/j.jngse.2016.11.041

Snell T, De Paola N, van Hunen J et al (2020) Modelling fluid flow in complex natural fault zones: Implications for natural and human-induced earthquake nucleation. Earth Planet Sci Lett 530:115869. https://doi.org/10.1016/j.epsl.2019.115869

Tanikawa W, Shimamoto T (2006) Klinkenberg effect for gas permeability and its comparison to water permeability for porous sedimentary rocks. Hydrol Earth Syst Sci Discuss 3:1315–1338

Walsh JB (1981) Effect of pore pressure and confining pressure on fracture permeability. Int J Rock Mech Min Sci Geomech Abstr 18:429–435. https://doi.org/10.1016/0148-9062(81)90006-1

Wang F, He J, Liang Y et al (2018) Study on the permeability characteristics of coal containing coalbed methane under different loading paths. Energy Sci Eng 6:475–483. https://doi.org/10.1002/ese3.221

Wang W, Duan X, Jia Y et al (2022) Deformation characteristics, gas permeability and energy evolution of low-permeability sandstone under cyclic loading and unloading path. Bull Eng Geol Env 81:369. https://doi.org/10.1007/s10064-022-02858-x

Wierzbicki M, Konečný P, Kožušníková A (2014) Permeability changes of coal cores and briquettes under tri-axial stress conditions. Arch Min Sci 59:1131–1140. https://doi.org/10.2478/amsc-2014-0079

Wu Y, PruessPersoff peter K (1998) Gas flow in porous media with Klinkenberg effects. Transp Porous Media 32:117–137. https://doi.org/10.1023/A:1006535211684

Yang J, Chen W, Yang D, Tian H (2017) Investigating the permeability of marble under moderate pressure and temperature. Geofluids 2017:1–8. https://doi.org/10.1155/2017/4126908

Zhang R, Ning Z, Yang F et al (2016) A laboratory study of the porosity-permeability relationships of shale and sandstone under effective stress. Int J Rock Mech Min Sci 81:19–27. https://doi.org/10.1016/j.ijrmms.2015.11.006

Zhang D, Yang Y, Wang H et al (2018) Experimental study on permeability characteristics of gas-containing raw coal under different stress conditions. R Soc Open Sci 5:180558. https://doi.org/10.1098/rsos.180558

Zhao Y, Cui D, Liu J et al (2021) Evolution of coal permeability under constant effective stresses: direct measurements and numerical modeling. Energy Fuels 35:15489–15501. https://doi.org/10.1021/acs.energyfuels.1c01425

Zhao F, Wei Y (2022) Regional characteristics of porosity and permeability of Dahebian syncline coal and its application. Front Earth Sci (Lausanne) 9. https://doi.org/10.3389/feart.2021.822322

Zheng J, Zheng L, Liu H-H, Ju Y (2015) Relationships between permeability, porosity and effective stress for low-permeability sedimentary rock. Int J Rock Mech Min Sci 78:304–318. https://doi.org/10.1016/j.ijrmms.2015.04.025

Zhijiao Z, Xiaochun L, Lu S et al (2014) Experimental study of the laws between the effective confining pressure and mudstone permeability. Energy Procedia 63:5654–5663. https://doi.org/10.1016/j.egypro.2014.11.598